

Reservoir Characterization of the Upper Part of Qamchuqa Formation from Miran and Bazian Oilfields in Kurdistan Region, NE Iraq

Danyar A. Salih^{1,*}, Fouad M. Qader¹

¹ Department of Geology, College of Science, University of Sulaimani, Kurdistan Region, Iraq

Keywords: Qamchuqa Formation; Porosity; Permeability; Hydrocarbon and Water Saturations; Hydrocarbon Movability.

ARTICLE INFO.

Article history:

-Received: 14 July 2023
-Received in revised form: 26 Aug. 2023
-Accepted: 27 Aug. 2023
-Final Proofreading: 24 Dec. 2023
-Available online: 25 Dec. 2023

Corresponding Author*:

Danyar A. Salih

danyar.salih@univsul.edu.iq

©2023 THIS IS AN OPEN ACCESS ARTICLE UNDER THE CC BY LICENSE
<http://creativecommons.org/licenses/by/4.0/>



ABSTRACT

Reservoir characterization of the upper part of Qamchuqa Formation at the wells of Miran West-2 (MW-2) and Bazian-1 (BN-1) is studied. This formation typically has low shale content at the BN-1 well. At the same time, in the MW-2 well, the middle part of the studied formation is dominated by shaly and shale intervals, possibly affected by the Sarmord and Balambo depositional environments. Although the upper part of Qamchuqa Formation is mainly composed of dolomite with minor dolomitic limestone, marl and shale are occasionally present. Furthermore, porosity values are commonly less than 15% in both wells; nevertheless, there are a few intervals where porosity significantly increases. The formation at the BN-1 well has a higher porosity than the MW-2 well. Moreover, the secondary porosity is relatively low as 4.0% at the MW-2 well, while in the well of BN-1, it ranges between < 4.0% and 7.5%. The measured permeability of the formation suggests good permeability. According to the shale volume, porosity, and permeability, the upper part of Qamchuqa Formation is subdivided into three reservoir units. RU 1 at the MW-2 well and RU 2 at the BN-1 well have the most substantial reservoir properties. However, the lowest reservoir quality appears within RU 1 of the BN-1 well and RU 2 at the well of MW-2. Additionally, residual hydrocarbons constitute an extensive fraction of the pore spaces, while tiny portions of the moveable one can be discovered along all reservoir units of the formation. Finally, considering the hydrocarbon movability of the MW-2 well, the upper part of Qamchuqa Formation is defined by primarily movable oils in RU 1 and 2. In contrast, moveable oils are detected in almost all of the reservoir units of the BN-1 well.

الصفات المكنية للجزء العلوي من تكوين القمچوقة في حقول مختارة، اقليم كوردستان، شمال شرق العراق

دانيار ابوبكر صالح، فؤاد محمد قادر

قسم علم الأرض، كلية العلوم، جامعة السليمانية، السليمانية، العراق

الملخص

تمت دراسة الخصائص المكنية للجزء العلوي من تكوين قمچوقة في البئر (MW-2) في حقل ميران و (BN-1) في حقل بازيان. اظهرت البيانات التي تم تحليلها أن التكوين ذو محتوى سجيلي منخفض في البئر BN-1، في حين إن منتصف المقطع في البئر MW-2 تهيم عليه منيات من السجيل وصخور الكاربونات السجيلي المتأثرة ببيئات ترسيب تكويني سارمورد وبالامبو؛ بينما يتكون باقي التكوين بشكل أساسي من محتويات منخفضة من الصخر السجيلي، و أشارت جميع البيانات المتعلقة إلى النتيجة ذاتها. يتكون التكوين بشكل أساسي من صخور الدولوميت مع الحجر الجيري الدولوميتي. علاوة على ذلك، تكون قيم المسامية عادة أقل من 10٪ في كلا البئرين؛ وهناك فترات قليلة تزداد فيها المسامية بشكل ملحوظ. يتميز التكوين في بئر BN-1 بمسامية أعلى من بئر MW-2، المسامية الثانوية تشكل تقريبا 40٪ في بئر MW-2، بينما في بئر BN-1 تتراوح ما بين 40٪ و 70٪. تشير النفاذية المقاسة للتكوين إلى نفاذية جيدة. تم تقسيم التكوين إلى ثلاث وحدات مكنية (RU1، RU2، RU3). يعتبر RU1 في بئر MW-2 و RU2 في بئر BN-1 بشكل منفصل على أنهما يمتلكان اهم الخصائص المكنية. على العكس من ذلك، اظهرت RU1 ادنى المواصفات المكنية في بئر BN-1 و RU2 في بئر MW-2، تشغل الهيدروكربونات المتبقية الثقيلة جزءا كبيرا من حجم المسامات، بينما يمكن ان يقدر الهيدروكربونات الخفيفة بكميات صغيرة على طول جميع وحدات الخزان في التكوين. أخيرًا، من ناحية الهيدروكربونات المتحركة، يهيم على التكوين أقل فترات من الهيدروكربونات المتحركة الفاعلة في RU2 و RU3 في بئر MW-2. علاوة على ذلك، يمكن اعتبار RU1 و RU2 نسبيًا وحدتان إنتاجيتان مقارنة بالوحدات الأخرى من نفس البئر. ومع ذلك، تم الكشف عن الهيدروكربونات المتحركة بشكل تقريبي في جميع وحدات المكن في البئر BN-1.

1. Introduction

Carbonate reservoirs in the Middle East maintain a substantial proportion of the conventional oil reserves, about 70%, and the majority are naturally fractured [1]. Iraq has potential petroleum basins and well-known hydrocarbon fields. In this regard, Kurdistan Region has been designated as a significant hydrocarbon province with dozens of oilfields of various sizes [2, 3]. In addition, because of its crucial contribution to the hydrocarbon accumulation in the petroleum system of the lower Cretaceous, unique consideration is given to the Qamchuqa Formation. The Qamchuqa Formation has been proven to be a potential reservoir rock in many oilfields, such as Miran, Taq Taq, Chamchamal, Khabbaz, and Kirkuk [3]. The Cretaceous rock successions are potential reservoir rocks in Iraq and the Kurdistan Region and include substantial productive reservoirs of Iraq's hydrocarbon reserves [4, 5]. Significant numbers of studies on the upper Qamchuqa Formation have been previously conducted; the following paragraphs represent a summary of some of them.

Al-Qayim et al. [3] determined the porosity and defined the dolomitization of the upper Qamchuqa Formation at Khabbaz oilfield. They demonstrated that the upper Qamchuqa reservoir can be classified into three units: A, B, and C. The reservoir units (B and C) were indicated as lower-quality units, while reservoir unit (A) was represented as the significant unit from a reservoir quality point of view.

Ghafur and Hasan [5] investigated the reservoir properties of the upper Qamchuqa Formation at Khabbaz oilfield. They indicated that the reservoir rock units of the formation are low in shale content and practically clean reservoirs. They subdivided unit (A) into six subunits. Meanwhile, unit (B) was subdivided into four subunits, and its quality was lower than unit (A). The determined porosity was compared with primary/sonic porosity. The porosity ranged from approximately 20% to 15% in units (A) and (B), respectively. The average water saturation was low within units (A) and (B), while the average hydrocarbon saturation was as high as 90%.

Al-Qayim and Rashid [6] performed research on the petrophysical analysis of the upper Qamchuqa reservoir in the Taq Taq oilfield to indicate the reservoir properties within the formation. They assessed porosity, permeability, residual and moveable hydrocarbons, and water saturation. In addition, the effects of microfacies and diagenesis on reservoir development were identified. They determined how fractures affected the upper Qamchuqa reservoir rocks and calculated the effective porosity. Accordingly, they divided the formation into three lithologic units.

Rashid et al. [7] studied the Qamchuqa Formation in the Miran west block. They concluded that the stratigraphic column referred to the Qamchuqa reservoir as not being significantly dolomitized as in the nearby outcrops. Moreover, they standardized the simple terminology for continuous vertical sections, from top to bottom, of the Kometan, Gulneri, Dukan, Qamchuqa, and Sarmord formations.

Daoud [8] determined the depositional setting and microfacies analysis of the Qamchuqa Formation at the Pira-Magroon area. Seven essential micro-facies were identified. The study demonstrated that the formation is affected by dolomitization merely in the upper part, while the middle and lower parts are not dolomitized and are rich in well-preserved micro-fossils. It suggested that shallow-water to open-marine settings were depositional environments of the Qamchuqa Formation, including inner ramp, middle-ramp, shoal, inter-tidal, lagoon, and sub-tidal.

Mahmood et al. [9] examined the distribution of bitumen and oil in the upper Qamchuqa condensate reservoir in the Khurmala oilfield. Data from three wells were used. The TOC content was applied to measure the amount of oil and bitumen within the formation. They proposed that the distribution of bitumen and oil in the gas zone was predominantly controlled by porosity, permeability, and fractures.

This study focuses on the reservoir characteristics of the upper part of Qamchuqa Formation at the wells of Miran West-2 (MW-2) and Bazian-1 (BN-1), including lithology, porosity, permeability, reservoir units, saturations, and movability of hydrocarbons.

1.1 The Study Area

The studied wells of MW-2 and BN-1 are located within the Miran and Bazian fields, respectively, in Kurdistan Region, NE Iraq. The Miran Field is situated to the northwest of Sulaimania City. The oilfield is on the western edge of the High-Folded-Zone from a tectonic viewpoint (Fig. 1), which extends from the southeast to the northwest [10, 11]. The ridge of Tasluja is a predominant downward topographic expression that can be discovered within the middle part of the Miran Field. The compression from the Tertiary has caused the western and eastern structures to reach their peak; at the Late Miocene, the compression is terminated through the thrusting phase [12]. Additionally, the surface expressions of the east and west structures within the Miran Field are non-considerable, as there is little surface evidence for these structures. It is believed that the most recent deposits have covered them [11, 12, 13, 14, 15]. Moreover, the Bazian Field is located to the north-west of Sulaimania City (Fig. 1). At the Bazian Field, the first exploration oil well is Bazian No. 1 (BN-1). The well is drilled to assess the hydrocarbon accumulations in the northern part of the Bazian field by the KNOC (Korea National Oil Corporation) company [16]. The Cretaceous formations consisting of the Shiranish, Kometan, and Qamchuqa formations are the major reservoir targets in the Bazian Field. While the second target of the reservoir is the formation of the upper Triassic and lower Jurassic. At the well of BN-1, the middle Cretaceous Kometan, Gulneri, and Qamchuqa formations are penetrated, whereas the Dukan Formation is missing [16, 17].

1.2 Geological Setting

Wetzel (1950) in [18] proposed the name of the formation as a Qamchuqa Limestone Formation and selected the type locality at the Qamchuqa Gorge North East of Iraq in Sulaimania Governorate. The earliest work of [18] has documented that the Qamchuqa Formation preserves a maximum thickness at the type section of about 750 m, where both boundaries of the formation are exposed. The overlying Kometan Formation and the Qamchuqa Formation's upper boundary are separated by an unconformable contact. However, the conformable and gradational contact with the Sarmord Formation indicates the lower boundary of the Qamchuqa Formation [19]. The thickness of the studied formation at the MW-2 and BN-1 wells is almost 280m and 150m individually. At the BN-1 and Miran East-1 wells, the occurrence of the Balambo Formation is possibly recognized in the upper part of Qamchuqa Formation. This stratigraphic relationship is predominantly comparable with the stratigraphy of the Zewe area, which demonstrates how the Balambo Formation interchanged with the Qamchuqa Formation [20]. Likewise, the lower part of Qamchuqa Formation indicates more significant interfingering relationships with the Sarmord Formation, particularly at Chamchamal-2 well and the wells of Kirkuk oilfield [21]. According to previous studies, the Qamchuqa Formation has been expanded to the status of Qamchuqa Group, including the upper Qamchuqa Formation, the upper Sarmord Formation and the lower Qamchuqa Formation (Fig. 2). The equivalent rock-units of the three Qamchuqa Group units are more distinguishable in southern and central Iraq, comprising Maudud Formation, Batiwah Formation and Shu'aiba Formation (Fig. 2) [22, 23].

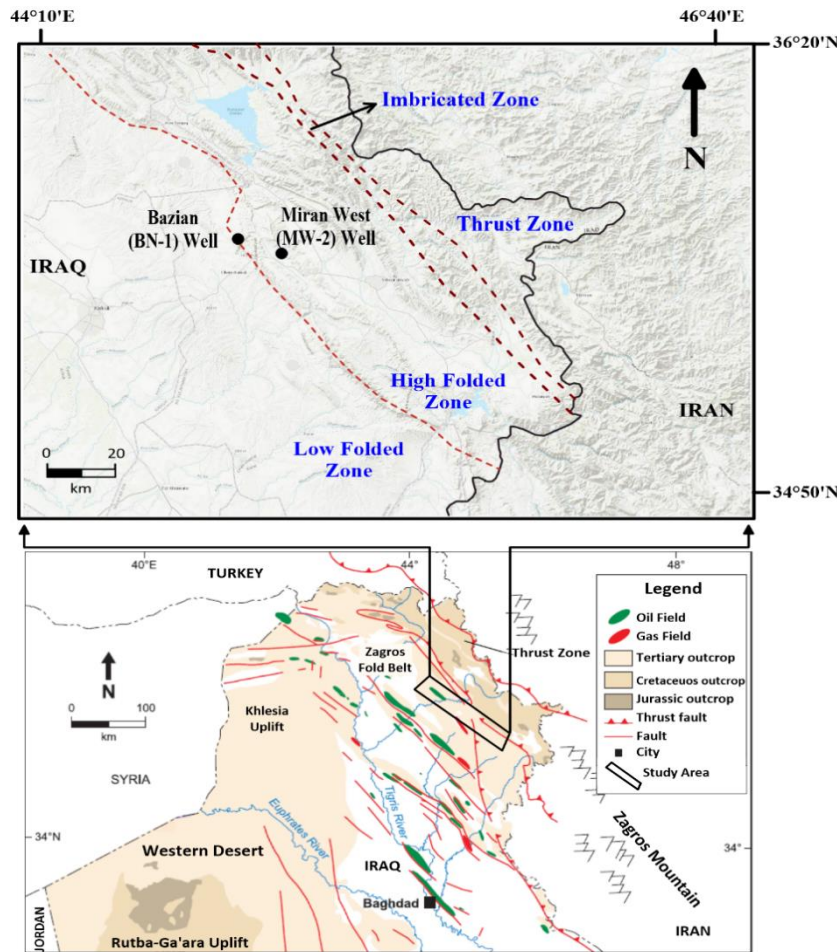


Fig. 1: Location of the studied wells and selected fields in the Iraqi structural provinces (modified after [3, 27])

The Qamchuqa Formation is mostly dominated by massive carbonates that have been extensively dolomitized. Here, six lithologic units can be distinguished within the formation at the type locality [19]. In Kirkuk city, most of the Qamchuqa Group units deposited along the Albian, defined by a relatively shallow-water platform, as well as numbers of inner-shelf facies are identified, including: lagoonal, dolostones, siliciclastics, evaporites, basinal and orbitolinid limestones with beds of marl [24, 25]. In Kurdistan Region and the south, central, and northwest of Iraq, the Qamchuqa Group's shelf-limestones are deposited and prograded eastwards over the Sarmord Formation which consists of slope-limestones and marl deposits, laterally graded to the Balambo Formation that comprises of the basinal-limestones [26]. Kurdistan Region, NE of Iraq, is in a fairly stable passive margin environment with confined extensional fault systems during the Early Cretaceous. As a result of the continuous passive margin setting, there is a long period of stable shelf environment, which permitted the deposition of a large amount of shallow marine rock-units. The reservoir rocks in the region have been formed from these sediments, since the majority of the rocks are carbonates of shallow marine limestones and dolomites [28].

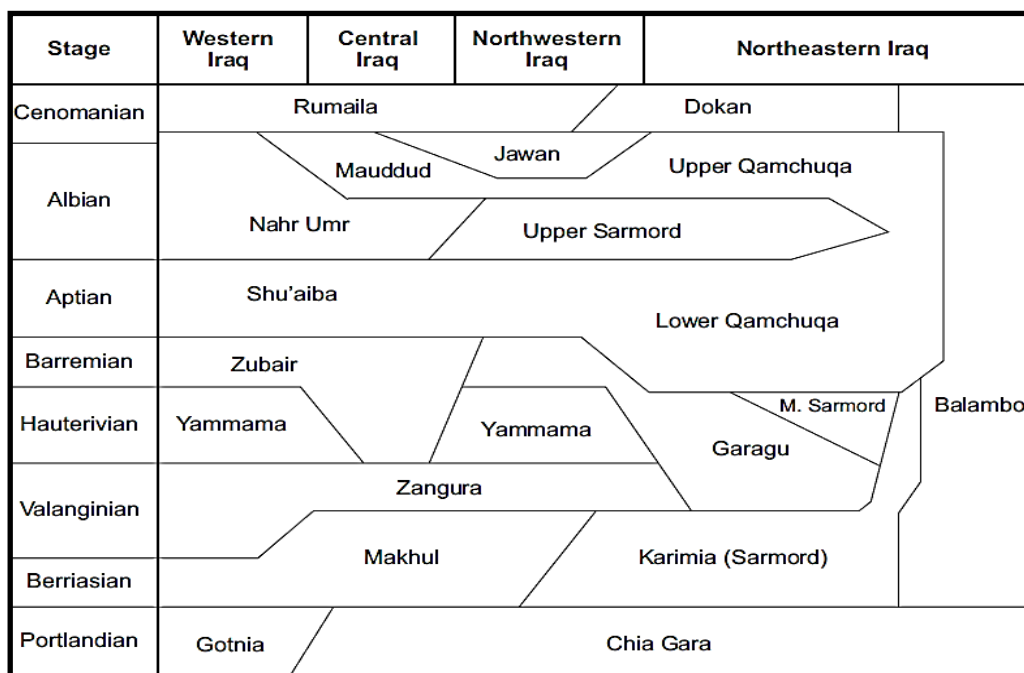


Fig. 2: The cretaceous rock-units across Iraq and Kurdistan Region in correlation with stratigraphic chart (after [3, 18])

2. Methods and Data

Wireline logs from two wells in the Miran and Bazian Fields were acquired from the Ministry of Natural Resources of Kurdistan Region, Iraq. The available logs were utilized to evaluate the petrophysical parameters of the upper part of Qamchuqa Formation in the MW-2 and BN-1 wells. Several logs, including the sonic log, density log, neutron log, and gamma-ray (GR) log, were used to define porosity, permeability, and lithology. To determine hydrocarbon and water saturations within the formation, resistivity logs of deep latero-log (LLD) and micro-spherical focused log (MSFL) were applied. To digitize the log sets, NeuraLog software was used, while Interactive Petrophysics software was utilized to analyze the data.

3. Results and Discussion

3.1 The Shale Volume

The shale volume was estimated in the formation under study by using (Equation 1 and 2) from the GR log data [29, 30]. The MW-2 well often records a higher GR value of the formation under study than the well of BN-1. In this regard, the maximum shale content in some intervals was around 50% and 60% at BN-1 and MW-2 wells, respectively (Fig. 3). Furthermore, the shale volume was used in order to identify intervals of the formation under study according to the classification of [31]. This approach indicates a clean interval where the shale content is less than 10%, while the shale volume between 10% to 35% of the rock unit defines a shaly zone. However, higher than 35% of shale content is a shale zone. Therefore, at MW-2 well, the upper part of Qamchuqa Formation was generally dominated by the shaly and shale zones between depths of 1400m and 1500m, while the rest of the formation was a clean zone apart from a few narrow intervals of shaly zones (Fig. 3). This reveals that the Qamchuqa Formation at the well of MW-2 progrades to the east over the Sarmord Formation, and laterally the Sarmord Formation passes over a short distance into the Balambo Formation [26]. Therefore, the Qamchuqa Formation at MW-2 well was more influenced by the slope and basinal depositional environments [20, 26]. In addition, the formation under study at the well of BN-1 is almost a clean formation as the shale volume is less than 10%, except few meters of shaly zones within the intervals of 2496m-2512m, and 2516m-2522m. In addition, the tiny narrow intervals of shaly zones were indicate along with intervals of 2375m-2377m, and 2523m-2525m (Fig. 3). Consequently, from the perspective of shale volume content, the studied formation at BN-1 well was relatively less shaly than in the well of MW-2.

$$I_{GR} = (GR_{Log} - GR_{Min}) / (GR_{Max} - GR_{Min}) \quad (1)$$

$$V_{Sh} = 0.33 (2^{2 \cdot I_{GR}} - 1.0) \quad (2)$$

Where:

I_{GR} : Index of gamma ray

GR_{Log}: Gamma ray value from log reading.
 GR_{Min}: Minimum value of GR in a clean zone.
 GR_{Max}: Maximum value of GR at shale zone.
 V_{Sh}= Volume of shale

3.2 Lithology

Several methods of lithological log descriptions were utilized to distinguish the lithology of the upper part of Qamchuqa Formation at the MW-2 and BN-1 wells based on the wireline well log data.

3.2.1 Neutron- Density (N-D) Cross-plot

The N-D cross-plot is a scheme between neutron porosity and formation density data. It is frequently applied to show the effects of lithology and porosity on various log responses [32]. Limestone, dolomites, sandstone and possibly anhydrite lithologies could be easily distinguished on such a cross-plot by considering the drilling fluid type [33]. The analysis of neutron porosity and bulk density from the N-D diagram revealed that the upper part of Qamchuqa Formation in the drilled wells of MW-2 and BN-1 significantly comprises dolomite and slightly dolomitic limestone as the data crossed near the lines of dolomite and limestone (Fig. 4). Additionally, the thin intervals of the shaly zones at the MW-2 well are indicated within the defined lithology of the studied formation (Fig. 4).

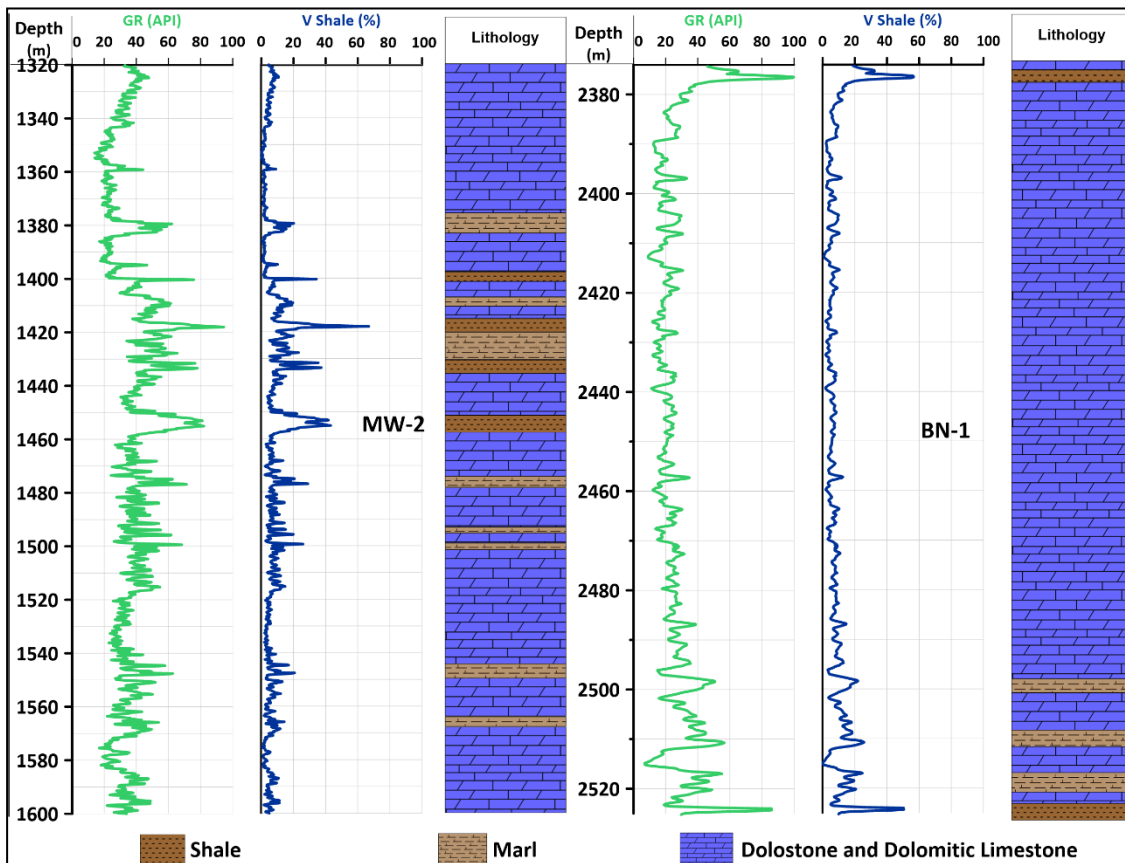


Fig. 3: GR log, the calculated volume of shale and lithology for the upper part of Qamchuqa Formation at the MW-2 and BN-1 wells

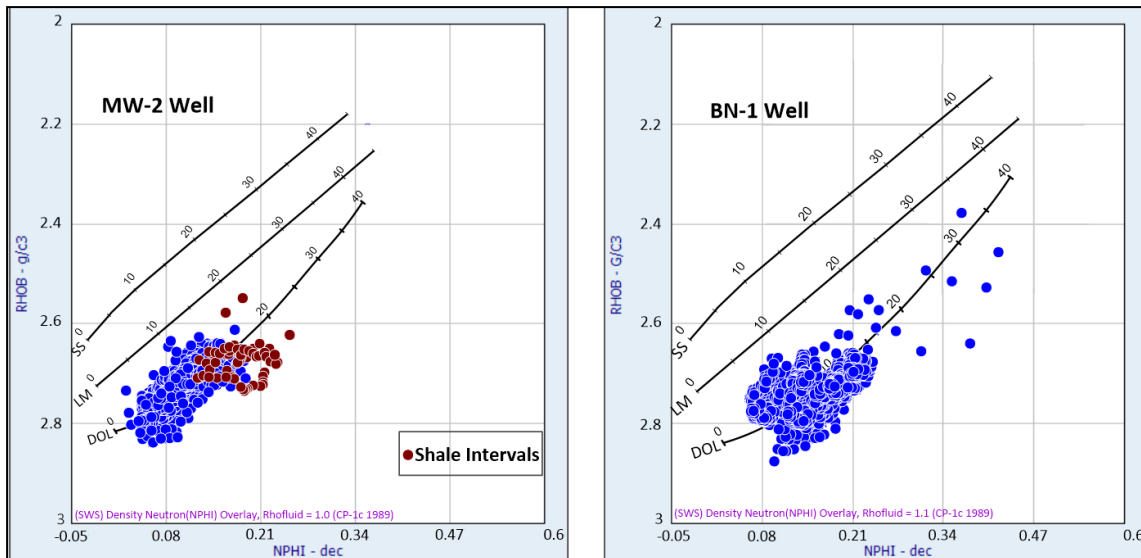


Fig. 4: N-D cross-plot of the upper part of Qamchuqa Formation in MW-2 and BN-1 wells, bulk density (RHOB) log in gm/cm³ and Neutron (NPHI) log in fraction (dec) (after [33])

3.2.2 Sonic-Neutron (S-D) Cross-plot

Sonic-Neutron (S-D) cross-plot uses the well-log data of neutron log and acoustic wave travel time log to identify different reservoir rocks. S-D cross-plot can be used to differentiate between a single reservoir lithology and shale rock, as well as to detect evaporite minerals [34]. In this concern, the available data of wireline well log was applied in order to understand the lithology types in the studied wells, as illustrated in figure (5). The analyzed data in the studied wells of BN-1 and MW-2 showed that the upper part of Qamchuqa Formation commonly consists of dolomite and minor dolomitic limestone (Fig. 5).

3.2.3 M-N Cross-plot

The approach of M-N cross-plot is dependent on the drilling fluid and response of log parameters that are effectively combined in the three porosity logs, which are sonic, density and neutron log techniques [32, 35]. According to [36], the M-N cross-plot can be applied in order to classify the mineral mixtures of complex lithology. Basically, M and N are the slopes of the lines on the cross-plots of sonic-density (S-D) and neutron-density (N-D) for the individual lithology separately. The M and N parameters are derived from Equations 3 and 4 [32], as follows:

$$M = [(\Delta t_f - \Delta t_{log}) / (\rho_b - \rho_f)] 0.01 \quad (3)$$

$$N = (\Delta N_f - \Delta N_{log}) / (\rho_b - \rho_f) \quad (4)$$

Where:

Δt_f : the sonic travel time of mud filtrate (fresh mud = 189 μ sec/ft and salt mud = 185 μ sec/ft)

Δt_{log} : the sonic log reading at any given depth in (μ sec/ft)

ρ_b : the bulk density of the matrix at any given depth in (gm/ cm³)

ρ_f : the fluid density (fresh mud = 1.0 gm/cm³ and salt mud = 1.1 gm/ cm³)

ΔN_f : the neutron of the fluid (100% porosity) in fraction and (generally = 1.0)

ΔN_{log} : the neutron porosity of the matrix at any given depth

0.01: the factor value that is used to scale the values of M parameter efficiently.

The abundance of the plotted data in the dolomite unit and slightly in calcite region clarified that dolomite with little dolomitic limestone is the dominant lithology of the upper part of Qamchuqa Formation in the studied wells (Fig. 6). Therefore, the lithology of the studied formation as determined by the M-N cross-plot was consistent with the consequences of the N-D and S-D cross-plot methods used in the MW-2 and BN-1 wells. Subsequently, the upper part of Qamchuqa Formation was evaluated lithologically from log descriptions using three various approaches. All of these approaches led to the same conclusion that this formation is primarily composed of dolomite that contains minor dolomitic limestone with very thin intervals of shale and marl lithology.

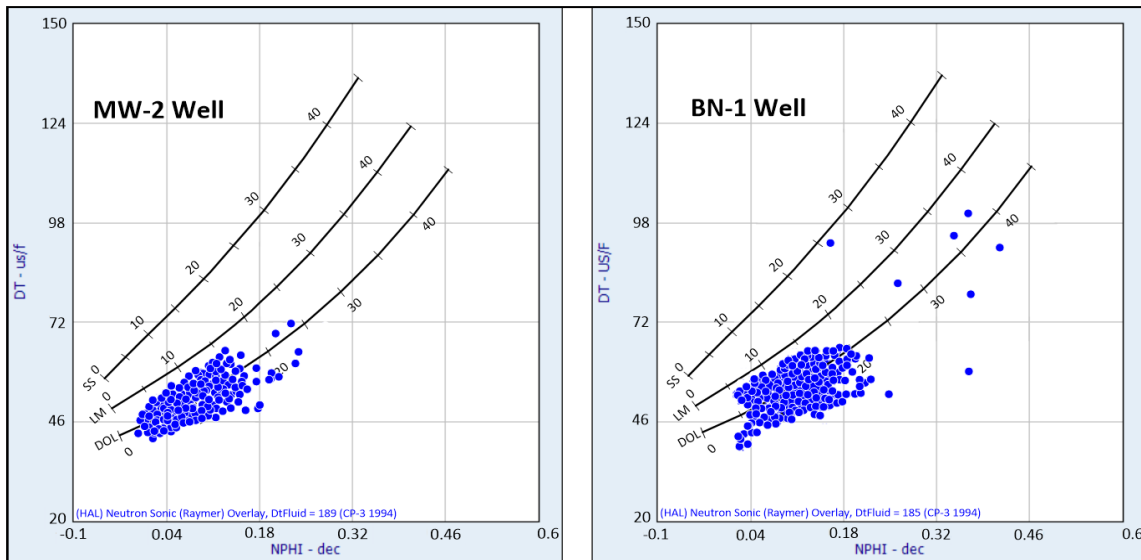


Fig. 5: S-D cross-plot of the upper part of Qamchuqa Formation in MW2 and BN-1 wells, Neutron (NPHI) log in fraction (dec) and acoustic wave travel time (DT) log in (Sonic Log) ($\mu\text{s}/\text{ft}$) (after [33])

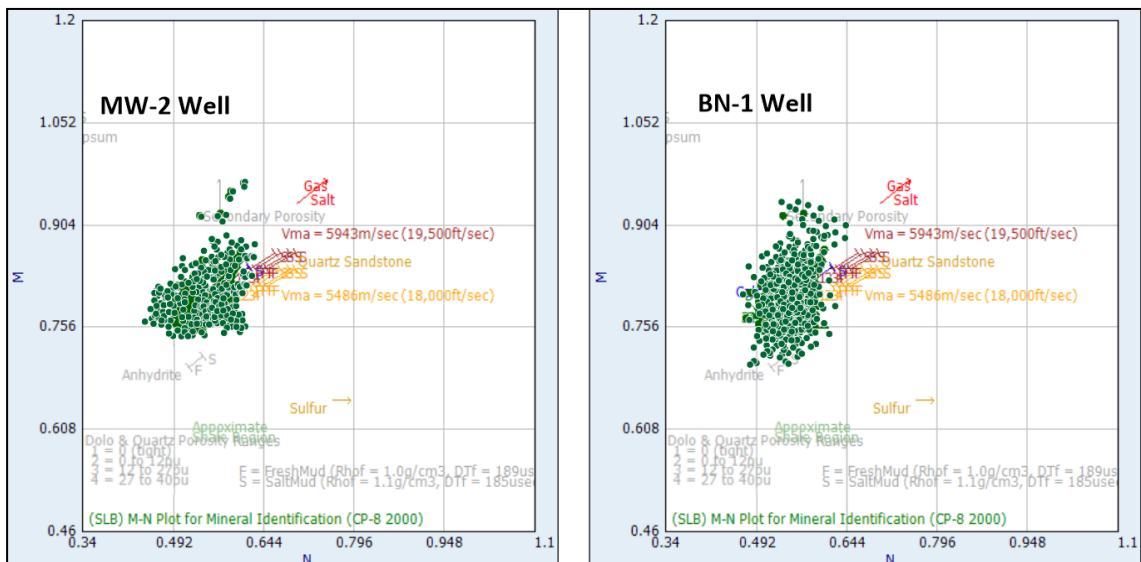


Fig. 6: M-N cross-plot of the upper part of Qamchuqa Formation in the studied wells (after [33])

3.3 Porosity

The presented primary and secondary porosities are sufficiently defined through the measured combination of neutron-density porosity (total neutron-density porosity). According to Schlumberger's technique [32], the neutron-density combination porosity ($\varnothing\text{N-D}$) was evaluated for the studied formation in the selected oilfields. The neutron-density porosity before and after correction from the shale volume was determined for the upper part of Qamchuqa Formation in the wells of MW-2 and BN-1 (Fig. 7). The average porosity values were recorded as 0.07 and 0.09 separately at MW-2 and BN-1 wells. However, the number of intervals in the MW-2 well had a higher porosity at depth zones of 1334-1336m, 1367-1368m, 1372-1373m, and 1407-1408m. At the BN-1 well, these horizons (2436-2437m, 2457-2458.5m, 2461-2462 m, and 2466-2467.5 m) were characterized by greater porosity records (Fig. 7). In general, at the MW-2 well, the average porosity was around 12.5% from the top to the middle of the studied formation and reduced downward to about 5.3%. Meanwhile at the BN-1 well, the average porosity of the upper part of Qamchuqa Formation remained essentially constant at around 8.2%, except for a few intervals where the porosity substantially increased to about 42% with an overall 4.0 m thick. Consequently, the calculated $\varnothing\text{N-D}$ indicated that the studied formation at BN-1 well had a higher porosity than the MW-2 well; the values on average were 9.0% and 7.0%, respectively.

3.4 Secondary Porosity

Primary and secondary porosities are the two different types of porosity that can be identified in reservoir rocks. The combination of corrected neutron-density porosity includes both primary and secondary porosities. The initial and distinct porosities that exist during deposition are referred to as primary porosity (matrix porosity). Moreover, secondary porosity is the consequence of post-depositional processes comprising fracture, re-precipitation, and dissolution. This demonstrates that secondary porosity is created when tectonic forces and the formation water come into contact and interact. Secondary porosity is mainly controlled by the diagenesis process. Additionally, summing up primary and secondary porosities yields the total porosity [37, 38, 39]. Since sonic porosity is usually used to indicate primary (matrix) porosity and neutron-density porosity is applied to determine total porosity; therefore, the difference among them ought to be utilized to quantify secondary porosity [29].

In the studied wells of MW-2 and BN-1, for estimating the proportions of secondary porosity for the upper part of Qamchuqa Formation, the variations between the corrected sonic porosity and the corrected neutron-density porosity were calculated, as shown in figure (8). Generally, the secondary porosity at the MW2 well decreased toward the bottom of the formation. Its value was less than 10% from the top to depth of 1390m, except certain intervals that did not exceed 6.0 m in total. Nonetheless, the majority of the formation in the MW-2 well was dominated by secondary porosity of about 4.0% with some horizons from a depth of 1400 m to 1460 m. The formation was characterized by a higher fraction of secondary porosity. Furthermore, the secondary porosity was distributed heterogeneously in the upper part of Qamchuqa Formation at the well of BN-1, whilst measurements of secondary porosity at the well of BN-1 commonly ranged from 4.0% to 7.5%. There were particular intervals where the secondary porosity was higher than 10% (Fig. 8). This is because of the location of BN-1 well, as it is situated at the crest of the structure [17].

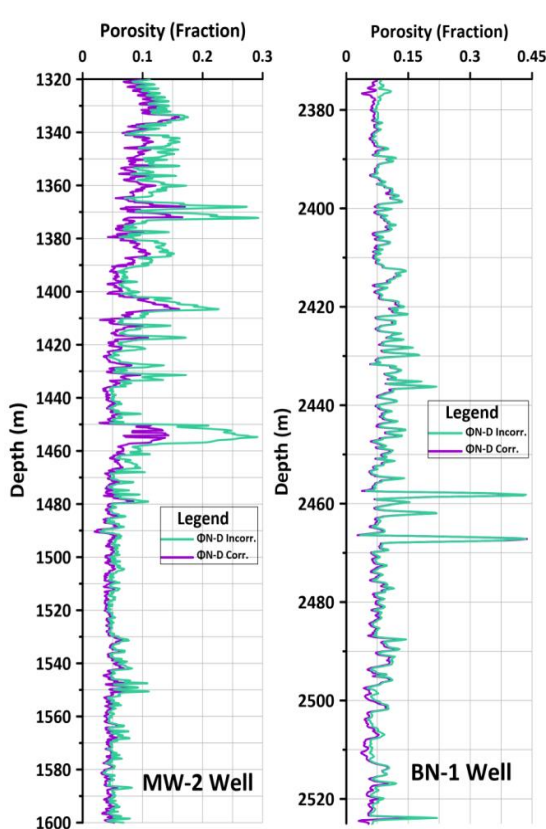


Fig. 7: Measuring the in-corrected and corrected neutron-density porosity from the impact of shale content for the studied formation at MW-2 and BN-1 wells

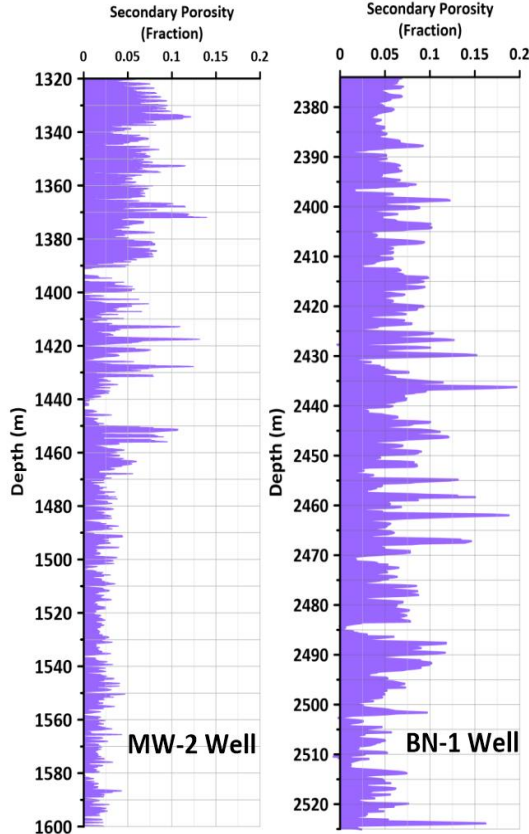


Fig. 8: Defining the secondary porosity for the upper part of Qamchuqa Formation in the wells of MW-2 and BN-1

3.5 Permeability

The capacity of a porous material to transmit fluids is known as permeability. Permeability determines how fluid may pass through a reservoir. Through core sample analysis and interpretation of in-situ measurements conducted by formation testers, such as well testing, core samples and well logging sets can all yield permeability data [32, 40]. An empirical formula of Wyllie and Rose [41] (Equation 5) was applied to determine the permeability (K Equation) of the studied formation in the wells of MW-2 and BN-1.

$$K = C*(\Theta)^3 / (S_{w_{irr}})^2 \quad (5)$$

Where:

K: Permeability determination from equation/ formula

C: Constant, which is hydrocarbons density dependent (for dry gas C=79 and for oil C=250)

Θ: Corrected neutron density porosity

S_{w_{irr}}: Irreducible water saturation

The more comprehensive approach for estimating permeability values from the given log data is the multivariable linear regression (MLR) method. Expected permeability values obtained from log data are considered dependent values, at the same time well-log data are recognized as independent values [42, 43]. The approach of MLR was applied to define the predicted permeability from well log data (K Log). This technique has recently been used by [44, 45]. In this study, two principles of multiple regression equations were applied in order to obtain a stronger correlation between the dependent permeability and log-derived permeability. The first principle was K Log1, including the independent parameters of gamma-ray (GR), acoustic travel time (DT), bulk density (pb) and neutron porosity (ΘN). Besides, the deep laterolog (LLD) measurement was involved in the second principle, namely K log2 [42, 46]. Measurement of permeability for the upper part of Qamchuqa Formation was acquired from Equations 6 and 7 separately (Fig. 9) at the wells of MW-2 and BN-1 as the strongest relationship between K Equation and K Log 1 and 2.

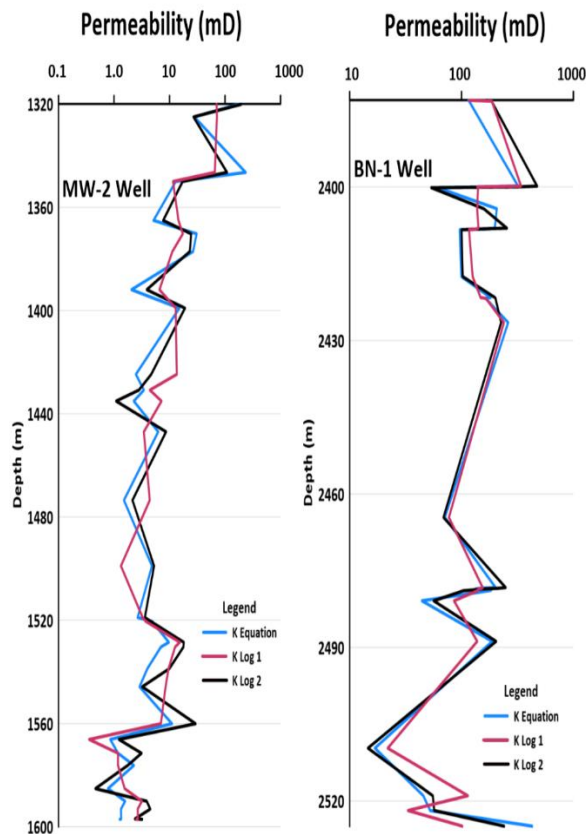


Fig. 9: The calculated permeability from equation (K Equation) and the determined permeability from MLR technique (K Log 1 and 2) for the upper part of Qamchuqa Formation in the MW-2 and BN-1 wells

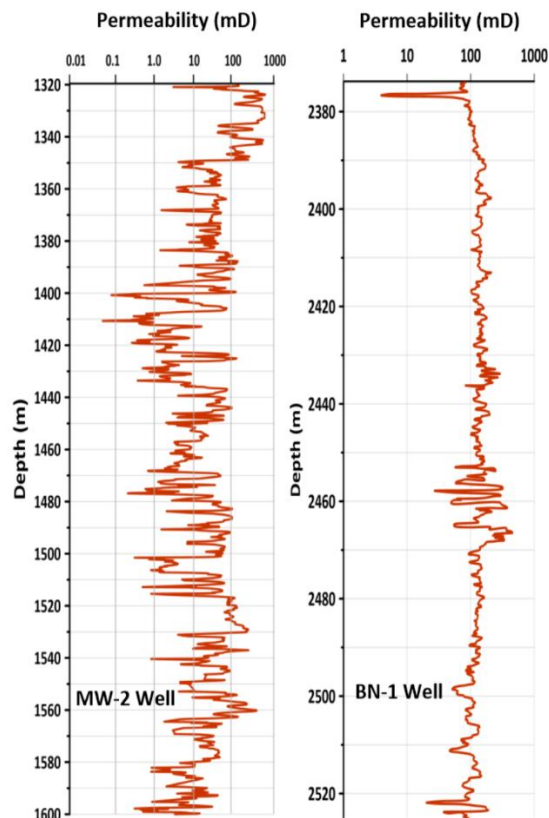


Fig. 10: The determined log for the derived permeability of the upper part of Qamchuqa Formation in the wells of MW-2 and BN-1

$$K = 1199.7 + (-4.182 * GR) + (1.562 * DT) + (-0.584 * pb) + (2.02 * \Theta N) + (0.099 * LLD) \quad (6)$$

$$K = 1255 + (-36.965 * GR) + (23.2582 * DT) + (-17.124 * pb) + (22.8145 * \Theta N) + (0.0349 * LLD) \quad (7)$$

Where:

K: Permeability estimation from log data (mD), GR: Gamma Ray (API), DT: acoustic travel time (μ.s/ft), pb: Bulk density (gm/cc), ΘN: Neutron porosity (Frac.), LLD: Deep Laterolog (ohm.m)

The obtained permeability from the MLR technique at the MW-2 well indicated higher permeability at the top and comparatively declining downward. The studied formation in this well had specific intervals of extremely high permeability among depths of 1322-1350m, 1520-1530m and 1552-1562m. In addition, in the BN-1 well, the defined permeability was roughly 100mD along the entire studied formation, while certain horizons within the formation along depths of 2453-2466m were predominated by extraordinarily high permeability zones (Fig. 10). Additionally, the defined permeability of the upper part of Qamchuqa Formation along the BN-1 well was generally greater than that of the MW-2 well, despite having much higher permeability intervals at the top of the MW-2 well. As a result, the permeability of the upper part of Qamchuqa Formation in both of the studied wells was relatively high and reflected good permeability [47].

3.6 Reservoir Units

To differentiate between units and perspectives of various reservoir properties, regardless of the stored fluid type within the reservoir, the identified major rock properties of shale volume, porosity and permeability of the studied formation were used. In the MW-2 and BN-1 wells, the reservoir units of the studied formations were distinguished according to the differences in the three aforementioned criteria. The upper part of Qamchuqa Formation was divided into three reservoir units in the MW-2 and BN-1 wells, as illustrated in Fig. 11.

The average, minimum and maximum data for porosity, shale content, permeability and depth intervals with the thickness of each recognized reservoir unit are given in Table 1. Consequently, RU 1 at the MW-2 well and RU 2 at the BN-1 well had the most significant reservoir characteristics. This is due to the lowest shale content and the highest average porosity and permeability values recorded along them. However, RU 1 at the BN-1 well and RU 2 at the MW-2 well, compared to the other units, seemed to have the least reservoir properties as the amount of shale volume was the highest; also, porosity and permeability were the lowest (Table 1).

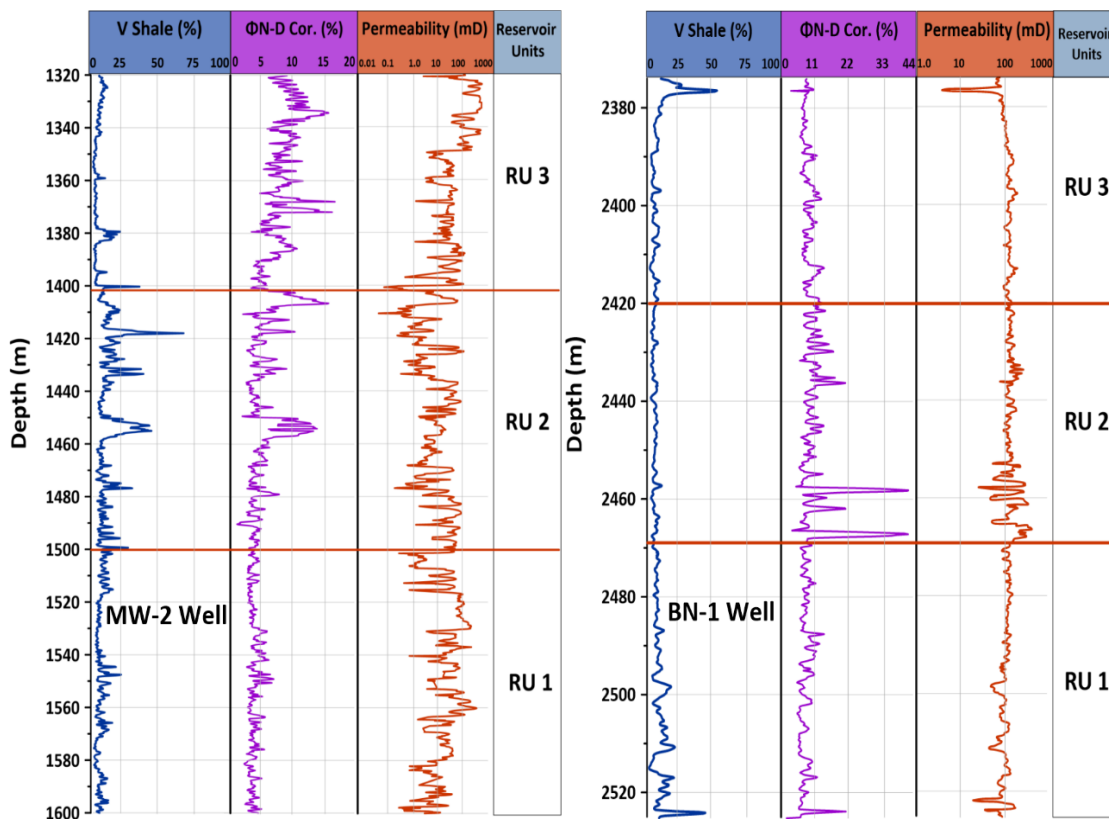


Fig. 11: The recognized reservoir units based on porosity, permeability and shale volume for the upper part of Qamchuqa Formation in the MW-2 and BN-1 wells

Table 1: Depth of the units and thickness, with a summary of parameters of the recognized reservoir units of the studied formation in the wells of MW-2 and BN-1

MW-2 Well						
Reservoir Units	Depth Interval (m)	Thickness (m)	Statistics	V shale (%)	Porosity (%)	Permeability (mD)
RU 3	1320-1401	81	Min	0	4	0.08
			Max	32	14	719
			Average	5	7	156
RU 2	1401-1500	99	Min	3	2	0.06
			Max	67	15	115
			Average	16	6	19.7
RU 1	1500-1600	100	Min	1	3	0.94
			Max	25	8	421
			Average	6	5	52.8
BN-1 Well						
Reservoir Units	Depth Interval (m)	Thickness (m)	Statistics	V shale (%)	Porosity (%)	Permeability (mD)
RU 3	2374-2420	46	Min	0	3	3.9
			Max	56	14	210.7
			Average	6	9	125.6
RU 2	2420-2469.5	49.5	Min	1	3	15.2
			Max	11	42	467.7
			Average	4	11	149.3
RU 1	2469.5-2525	55.5	Min	0	1	20.1
			Max	48	20	190.5
			Average	1	8	101.8

3.7 Water and Hydrocarbon Saturations

Water saturation contributes significantly to reservoir evaluations. Depending on the porosity, water saturation, and reservoir capacity, the oil saturation in any reservoir can be calculated. Multiple techniques enable the determination of water saturation, including direct assessment of core samples, capillary pressure data and Archie's equation [29, 48]. The water saturation estimation through Archie's equation required the cementation factor (m) value, which was obtained utilizing Pickett cross-plot approach, recorded as 1.91 and 1.78 in the MW-2 and BN-1 wells, respectively (Fig. 12). Readings from the resistivity logging tools were used to indicate the values of R_{xo} and R_t , including the micro-spherical focused log (MSFL) and deep latero-log (LLD) correspondingly. According to [49], the water and hydrocarbon saturations in the studied formation were defined by using Equations 8 and 9. Water saturation measurements within the flushed (S_{xo}) and uninvaded zones (S_w) contributed to estimating the moveable oil/hydrocarbon saturations (MOS) and residual oil/hydrocarbon saturations (ROS). The mentioned parameters were individually computed by using Equations 10- 12 [48, 49].

$$\text{Water saturation of uninvaded zone } (S_w) = [(a * R_w) / (R_t * \Phi^m)]^{1/n} \quad (8)$$

$$\text{Hydrocarbon saturation } (S_h) = 1 - S_w \quad (9)$$

$$\text{Water saturation of the flushed zone } (S_{xo}) = [(a * R_{mf}) / (R_{xo} * \Phi^m)]^{1/n} \quad (10)$$

$$\text{Moveable oil/hydrocarbon saturation (MOS)} = S_{xo} - S_w \quad (11)$$

$$\text{Residual oil/hydrocarbon Saturation (ROS)} = 1 - S_{xo} \quad (12)$$

Where:

- a: Tortuosity factor (is equal to 1.0 for the carbonate rocks).
- R_w : Resistivity of the formation water at the formation temperature.
- R_t : True formation resistivity from LLD.
- R_{mf} : Resistivity of the mud filtrate at the formation temperature.
- R_{xo} : Shallow resistivity from MSFL.
- Φ : Obtained porosity from logs.
- m: Cementation exponent/factor.
- n: saturation exponent (it is assumed to be 2.0).

Together, moveable and residual hydrocarbons, were included in the hydrocarbon saturation of the formations. The first hydrocarbon was recoverable hydrocarbons that can be produced, whilst the last one was trapped in reservoirs and cannot be extracted. Equations 13- 16 propose that the saturation parameters can be expressed as a percentage within the pore spaces, i.e. demonstrate them as volume fractions that confined inside the porosity [50,51].

$$\text{Bulk volume of water saturation } (S_w) = S_w * \Phi \quad (13)$$

$$\text{Bulk volume of hydrocarbon saturation } (S_h) = (1 - S_w) * \Phi \quad (14)$$

$$\text{Bulk volume of moveable oil saturation (MOS)} = (S_{xo} - S_w) * \Phi \quad (15)$$

$$\text{Bulk volume of residual oil saturation (ROS)} = (1 - S_{xo}) * \Phi \quad (16)$$

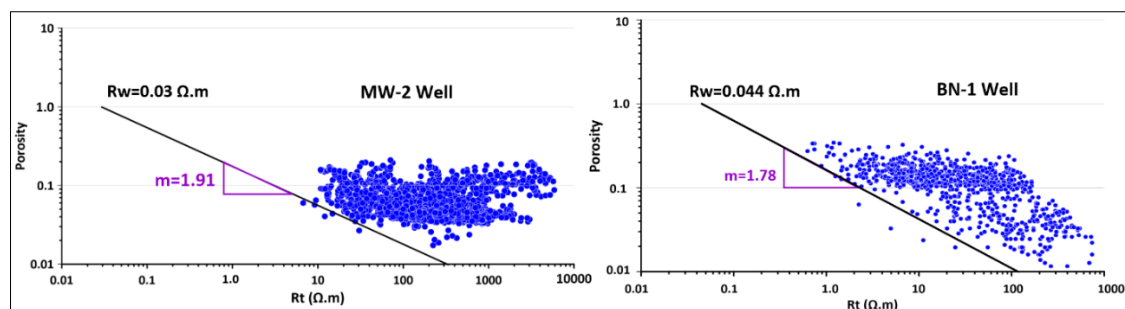


Fig. 12: The cementation factor (m) from Pickett cross-plot for the upper part of Qamchuqa Formation in the wells of MW-2 and BN-1

In the studied wells of MW-2 and BN-1, the aforementioned saturations were distributed within the porosity of the upper part of Qamchuqa Formation (Fig. 13). A trace quantity of moveable hydrocarbon could be detected with all of the defined reservoir units of the studied formation in both wells. In contrast, the majority of the hydrocarbons were of the residual type in the MW-2 and BN-1 wells. Considering water saturation, the MW-2 well had a higher proportion of water saturation than the well of BN-1, which had the lowest fraction (Fig. 13). Additionally, in the studied formation, a combination of the significant amounts of residual hydrocarbon saturation and comparatively high porosity proposed the occurrence of isolated and tiny pores. Accordingly, the upper part of Qamchuqa Formations' pore spaces was dominated by the residual hydrocarbon saturation in majority. As previously noted, the RU 1 and RU 2 individually in the MW-2 and BN-1 wells had the best reservoir quality; so, a certain volume of moveable oil was detected there. Then, within the upper part of Qamchuqa Formation, the higher concentration of water saturation was generally associated with a greater volume of shale content at the MW-2 well. As previously mentioned, the porosity and permeability at the BN-1 well had comparatively higher average values than in the MW-2 well. Consequently, a higher percentage of moveable and residual hydrocarbons was recorded with less water saturation at the well of BN-1 as compared to the MW-2 well (Table 1).

3.8 Moveable Hydrocarbon Index

One of the quick-look techniques for assessing hydrocarbon movability is the Moveable Hydrocarbon Index (MHI). Thus, MHI can be employed to decide the hydrocarbon occurrence and movability in the reservoir. Hydrocarbon mobility may be computed utilizing the calculated values of both water saturations in the flushed zone (S_{xo}) and the uninvaded zone (S_w); therefore, the MHI value is estimated from the ratio of S_w/S_{xo} [52]. When the obtained data of S_{xo} exceeds S_w , this indicates that the hydrocarbons in the flushed zone are probably displaced or flushed out of the zone closest to the borehole as a result of the drilling fluids invasion [49]. When the measured MHI values are equal to 1.0 or above, it means that during the invasion there are no mobile hydrocarbons occurred. This is true regardless whether the intervals include hydrocarbons or not [52, 53]. Furthermore, wherever the MHI ratio is less than 0.6 and 0.7 for limestones and sandstones respectively, it is an indication of the moveable hydrocarbons occurrence. Once a reservoir has an MHI below 0.6, it suggests that the hydrocarbons have enough permeability to move during the mud filtration through the invasion process [53].

In the studied wells, the obtained MHI ratio for the upper part of Qamchuqa Formation and its reservoir units are illustrated in figure (14). Since the studied formation composed of carbonate rocks as proved in this study, the value of 0.6 is typically utilized as an MHI cutoff for the carbonate reservoirs to distinguish moveable and non-moveable hydrocarbon zones [52]. The upper part of Qamchuqa Formation in the MW-2 well, particularly in RU1 and RU2, contained mostly moveable hydrocarbons with a few thin horizons of non-moveable oil. Besides, in unit 3, the studied formation was predominant with the least effective zones of moveable oil compared to the other units. Consequently, from most to least effective hydrocarbon intervals, the reservoir units of the upper part of Qamchuqa Formation in the well of MW-2 can be classified as follows: RU 1, RU 2, and lastly RU 3 (Fig. 14). Moreover, in the studied well of BN-1, moveable hydrocarbons occurred in nearly all of the reservoir units along the formation. However, not all of the units contained effective moveable hydrocarbons and also had merely a few intercalated narrow intervals of non-moveable oil with various thicknesses. The defined permeability of the studied formation was higher at the BN-1 well compared to the MW2 well; therefore, more moveable hydrocarbons existed along the BN-1 well.

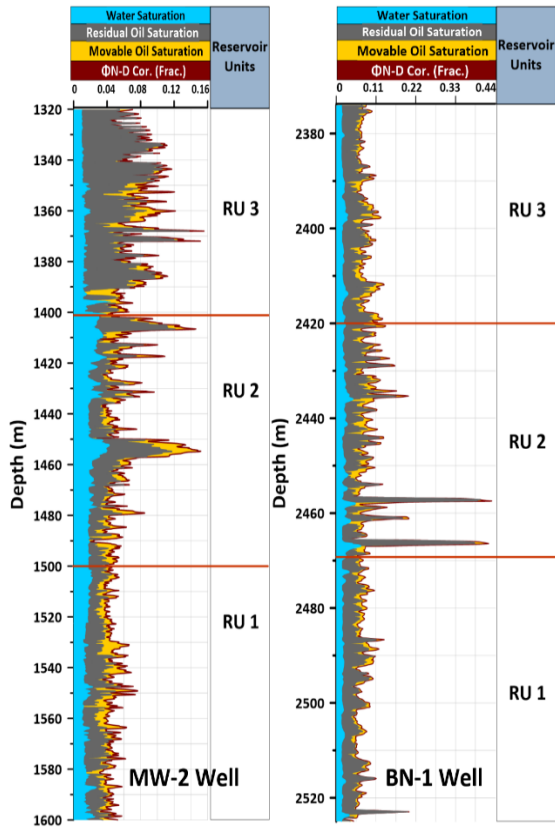


Fig. 13: Water saturation and oil saturation (moveable and residual) for the upper part of Qamchuqa Formation in the studied wells

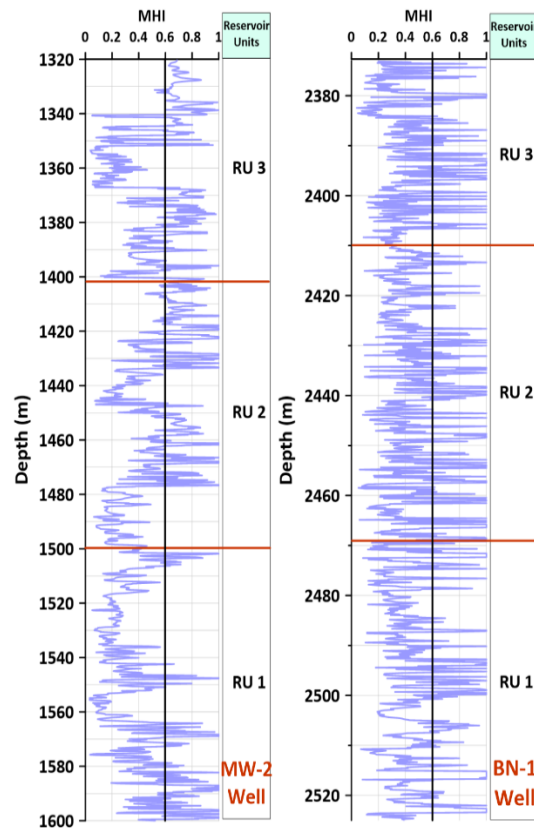


Fig. 14: Measured Moveable Hydrocarbon Index for the Upper part of the studied formation in the wells of MW-2 and BN-1

Conclusions

The following are the main conclusions of the study:

- The ratio of defined shale volume is commonly low at the upper part of Qamchuqa Formation. The low shale zones (<10%) represent the majority of the formation at the well of MW-2. However, a few thin intervals in the middle of the MW-2 well predominate in shaly and shale zones. This is resulted from the interchanging depositional environments of the Sarmord and Balambo Formations with the Qamchuqa Formation. Moreover, at the BN-1 well, the studied formation primarily comprises low shale content.
- The studied formation in the selected wells is primarily composed of dolomite, including some dolomitic limestone with horizons of shale and marl.
- Porosity is obtained through the sonic log, with density and neutron logs. The results propose that the porosity is typically about 5% to 13% in the MW-2 and BN-1 wells. Additionally, the upper part of Qamchuqa Formation in the BN-1 well has a greater porosity than the well of MW-2. However, there are only a few zones where porosity highly increases. The estimated secondary porosity supports that the studied formation has more secondary porosity along the BN-1 well than the MW-2 well.
- The observed permeability of the upper part of Qamchuqa Formation points to good permeability in the studied wells.
- The formation is divided into three reservoir units according to the measured shale volume, porosity, and permeability. The RU 1 in the MW-2 well and RU 2 in the well of BN-1 are recognized as having the most significant reservoir qualities among the distinguished reservoir units. Extensive portions of shale volume with lower porosity and permeability ratios have resulted in the lowest reservoir properties being discovered along the RU 1 and RU 2 in the wells of BN-1 and MW-2, respectively.

- A little quantity of moveable hydrocarbons can be detected amongst all reservoir units. The residual oils make up a significant component of the pore spaces of the formation. The upper part of Qamchuqa Formation in the MW-2 well has a greater water saturation in comparison to the well of BN-1.
- According to hydrocarbon movability, RU 2 and RU 3 are predominated by the least productive portions of moveable oil. Moreover, RU 1 and 2 may be regarded as more productive intervals than the other units of the formation in the MW-2 well. In the well of BN-1, nearly all reservoir units have productive moveable oils, although it appears in a tiny portion.

Acknowledgement

The authors would like to express their gratitude and sincere appreciation to the Ministry of Natural Resources in Kurdistan Region of Iraq for providing data for the research.

References

- [1] Aljuboory, F.A. et al. (2020). Effect of fracture characteristics on history matching in the Qamchuqa reservoir: a case study from Iraq. *Carbonates and Evaporites*, 35, pp.1-20.
- [2] Buday, T. (1980). *The Regional Geology of Iraq, Vol 1: Stratigraphy and Paleogeography*. Publications of Geological Survey of Iraq, Baghdad, 445 p.
- [3] Al-Qayim, B., Qadir, F. and Al-Biati, F. (2010). Dolomitization and porosity evaluation of the cretaceous upper Qamchuqa (Maudud) formation, Khabbaz oilfield, Krikuk area, northern Iraq. *GeoArabia* 15, 49–76.
- [4] Hakimi, M.H. and Najaf, A.A. (2016). Origin of crude oils from oilfields in the Zagros Fold Belt, southern Iraq: Relation to organic matter input and paleoenvironmental conditions. *Marine and Petroleum Geology*, 78, pp.547-561
- [5] Ghafur, A.A. and Hasan, D.A. (2017). Petrophysical properties of the upper qamchuqa carbonate reservoir through well log evaluation in the Khabbaz oilfield. *Journal of Science and Engineering*, 1(1), pp.72-88.
- [6] Al-Qayim, B. and Rashid, F. (2012). Reservoir characteristics of the albian upper qamchuqa formation carbonates, taq taq oilfield, Kurdistan, Iraq. *Journal of Petroleum Geology*, 35(4), pp.317-341.
- [7] Rashid, F. et al. (2020). Characterization and impact on reservoir quality of fractures in the Cretaceous Qamchuqa Formation, Zagros folded belt. *Mar. Petrol. Geol.* 113, 104–117.
- [8] Daoud, H.S. (2021). Microfacies analysis, depositional setting, and microfossil assemblages of Qamchuqa Formation (Early Cretaceous) in Piramagroon mountains, Sulaymaniyah Governorate, northeastern Iraq. *Arabian Journal of Geosciences*, 14(8), pp.1-16.
- [9] Mahmood, B.S. et al. (2022). Total organic carbon (TOC) contents and distribution within Upper Qamchuqa gas condensate Reservoir-Kurdistan Region of Iraq. *Arabian Journal of Geosciences*, 15(8), p.689.
- [10] Addendum to Geological Well Proposal Appraisal Well Miran West-2 (2010). On The Miran West Structure Miran Block, Zagros Fold Belt, Kurdistan Region, Iraq 22nd March.
- [11] Heritage report (2012). Project Ref: ECV1851.
- [12] Al-Hakari, S. H. S. (2011). Geometric analysis and structural evolution of NW Sulaimani area, Kurdistan Region, Iraq, Ph.D. dissertation, University of Sulaimani, Kurdistan Region, Iraq.
- [13] Kubli, T.E. (2013). Deformation history and thin-skinned vs. thick-skinned tectonics in the Zagros fold and Thrust Belt of southeastern Kurdistan. In *Hydrocarbon Exploration in the Zagros Mountains of Iraqi Kurdistan and Iran*, Geological Society Conference, Burlington House, Piccadilly.
- [14] Mohialdeen, I.M. et al. (2018). Biomarker analysis of the upper Jurassic Naokelekan and Barsarin formations in the Miran Well-2, Miran oil field, Kurdistan region, Iraq. *Arabian Journal of Geosciences*, 11, pp.1-15.
- [15] Salih, D.A. et al. (2020). Sterane biomarker analysis of Sargelu Formation, Miran West Field, MW-2 well, Kurdistan Region, NE Iraq: Implications for origin of organic matter, palaeoenvironment and maturity. *Journal of Zankoy Sulaimani- Part A*, 22(1), pp. 321-344.
- [16] Darwesh, A.K. (2014). RIH intermediate section casing in Bazian-1 exploration oil well. *WIT Transactions on Ecology and the Environment*, 186, pp.559-569.
- [17] Darwesh, A.K. (2020). Parameters optimization of oil well drilling operation (Doctoral dissertation, Luleå University of Technology).
- [18] Bellen, R.C. et al. (1959). *Iraq. Lexique Stratigraphique International III, Asie; Fasc. 10 a. Geol. Congr. Comm. Stratigr., Centre Nat. Recherche, Paris*, 333 p.
- [19] Jassim, S.Z. and Goff, J.C. eds. (2006). *Geology of Iraq. DOLIN*, distributed by Geological Society of London.
- [20] Al-Qayim, B. et al. (2016). Integrated stratigraphic study of the Cretaceous petroleum-potential succession, Sulaimani area, Kurdistan, Iraq. *Journal of Zankoy Sulaimani, Special Issue, GeoKurdistan II*, pp.395-428.
- [21] Al Shdidi, S., Thomas, G. and Delfaud, J. (1995). Sedimentology, diagenesis, and oil habitat of Lower Cretaceous Qamchuqa Group, northern Iraq. *AAPG bulletin*, 79(5), pp.763-778.

- [22] Al-Sadooni, F.N. (1978). Sedimentology and Petroleum Prospects of the Qamchuqa Group-Northern Iraq. Ph.D. Thesis (unpublished). University of Bristol, pp. 367.
- [23] Sadooni, F.N. and Aqrabi, A.A. (2000). Cretaceous sequence stratigraphy and petroleum potential of the Mesopotamian Basin, Iraq.
- [24] Dunnington, H.V. (1958). Generation, migration, accumulation, and dissipation of oil in northern Iraq: Middle East. Reprinted from AAPG Memoir by GeoArabia, 10, 2, 2005.
- [25] Al-Juboury, A., Al-Zoobay, B. and Al-Juwainy, Q. (2006). Facies analysis of the Albian-Cenomanian carbonates, northeastern Iraq. Earth and Life, 1, pp.1-14.
- [26] Aqrabi, A. et al. (2010). The petroleum Geology of Iraq. Scientific press Ltd. ed: Beaconsfield UK.
- [27] Buday, T. and Jassim, S.Z. (1987). The regional geology of Iraq, vol. 2: tectonism, magmatism and metamorphism. GEOSURV, Baghdad, 352pp.
- [28] Jassim, S. Z. and Buday, T. (2006). Units of the Unstable Shelf and the Zagros Suture, Chapter 6, in: Jassim, S. Z., and J.C. Goff, eds., "Geology of Iraq", first edition: Brno, Czech Republic, Prague and Moravian Museum, pp. 71-83.
- [29] Asquith, G.B. and Gibson, C.R. (1982). Basic well log analysis for geologists.
- [30] Dewan, J.T. (1983). Essentials of modern open-hole log interpretation: PennWell Publishing Company, Tulsa, Oklahoma, 361 p.
- [31] Ghorab, M., A. M. Ramadan and A. Z. Noh (2008). The Relation Between Shale Origin (Source or non-Source) and its Type for Abu Roash Formation at Wadi El-Natron Area, South of Western Desert, Egypt", Australian Journal of Basic Applied Sciences, 2 (3): 360-371.
- [32] Schlumberge (1989). Cased Hole Log Interpretation: Principles/applications. Schlumberger Educational Services.
- [33] Schlumberger (2009). Log interpretation charts. Sugar land Texas 77478.
- [34] Radwan, A.E. (2018). New petrophysical approach and study of the pore pressure and formation damage in Badri, Morgan and Sidki fields, Gulf of Suez region, Egypt., PhD Thesis, <https://doi.org/10.13140/RG.2.2.26651.82727>.
- [35] Bateman, R.M. (1985). Open hole log analysis and formation analysis.
- [36] Schlumberger (1997). Log Interpretation charts. Schlumberger Ltd. Houston, texas: 77252-2175.
- [37] Choquette, P.W. and Pray, L.C. (1970). Geologic nomenclature and classification of porosity in sedimentary carbonates. AAPG bulletin, 54 (2), pp.207-250.
- [38] Baker Hughes (1992). Advanced Wire line and MWD Procedure Manual, Houston.
- [39] Yue, D. et al. (2018). Reservoir quality, natural fractures, and gas productivity of upper Triassic Xujiahe tight gas sandstones in western Sichuan Basin, China. Marine and Petroleum Geology, 89, pp.370-386.
- [40] Selley, R.C. (1998). Elements of petroleum geology. Gulf Professional Publishing.
- [41] Wyllie, M.R.J. and Rose, W.D. (1950). Application of the Kozeny equation to consolidated porous media. Nature, 165(4207), pp.972-972.
- [42] Mohaghegh, S., Balan, B. and Ameri, S. (1997). Permeability determination from well log data. SPE formation evaluation, 12(03), pp.170-174.
- [43] Taghavi, A.A. (2005). Improved permeability estimation through use of fuzzy logic in a carbonate reservoir from southwest, Iran. In SPE Middle East Oil and Gas Show and Conference. OnePetro.
- [44] Baban, D.H. and Ahmed, S.M. (2021). Reservoir Properties of the Upper Oligocene-Lower Miocene Ibrahim Formation in the Garmian Area, Iraqi Kurdistan Region. Tikrit Journal of Pure Science, 26(6), pp.40-58.
- [45] Baban, D.H. and Ahmed, M.M. (2021). Characterization of the Carbonate Reservoir Unit A of the Upper Triassic Kurra Chine Formation in the well SH-4, Shaikan Oilfield, Iraqi Kurdistan Region, Using Wireline Log Data. Tikrit Journal of Pure Science, 26(2), pp.71-87.
- [46] Rafik, B. and Kamel, B. (2017). Prediction of permeability and porosity from well log data using the nonparametric regression with multivariate analysis and neural network, Hassi R'Mel Field, Algeria. Egyptian journal of petroleum, 26(3), pp.763-778.
- [47] North, F.K. (1985). Petroleum Geology, Allen and Unwin Inc., Boston, 607 p.
- [48] Rider, M. (1996). The geological interpretation of well logs, 2nd. ed. Rider French Consulting Ltd. Aberdeen, Sutherland. 178 pp.
- [49] Asquith, G. B. and D. Krygowski (2004). Chapter 1: Basic relationship of well log Interpretation in Basic Well Log Analysis, AAPG Methods in Exploration 16, Tulsa, Oklahoma
- [50] Serra, O. (1984). Fundamentals of Well Log Interpretation: the acquisition of well logging data, Singapore.
- [51] Rider, M. (2002). The Geological Interpretation of Well Logs, Second Edition, Rider French Consulting Ltd., Aberdeen and Sutherland.
- [52] Schlumberger (1972). Log Interpretation Manual/Principles. Vol. 1. Schlumberger Well Services Inc., Houston.
- [53] Asquith, G.B. (1985). Handbook of log evaluation techniques for carbonate reservoirs. AAPG, Tulsa, Oklahoma, USA.